CrossMark

Solar Energetic Particle Events with Protons Above 500 MeV Between 1995 and 2015 Measured with SOHO/EPHIN

P. Kühl[1] ⓘ · **N. Dresing**[1] · **B. Heber**[1] · **A. Klassen**[1]

Abstract The Sun is an effective particle accelerator that produces solar energetic particle (SEP) events, during which particles of up to several GeVs can be observed. These events, when they are observed at Earth with the neutron monitor network, are called ground-level enhancements (GLEs). Although these events with their high-energy component have been investigated for several decades, a clear relation between the spectral shape of the SEPs outside the Earth's magnetosphere and the increase in neutron monitor count rate has yet to be established. Hence, an analysis of these events is of interest for the space weather and for the solar event community.

In this article, SEP events with protons accelerated to above 500 MeV were identified using data obtained with the *Electron Proton Helium Instrument* (EPHIN) onboard the *Solar and Heliospheric Observatory* (SOHO) between 1995 and 2015. For a statistical analysis, onset times were determined for the events and the proton energy spectra were derived and fitted with a power law.

As a result, we present a list of 42 SEP events with protons accelerated to above 500 MeV measured with the EPHIN instrument onboard SOHO. The statistical analysis based on the fitted spectral slopes and absolute intensities is discussed, with special emphasis on whether an event has been observed as a GLE. Furthermore, we are able to determine that the derived intensity at 500 MeV and the observed increase in neutron monitor count rate are correlated for a subset of events.

Keywords Solar cosmic rays · Ground level enhancement · Solar energetic particles

1. Introduction

The first solar energetic particle (SEP) event, which is now called a ground-level enhancement (GLE), was reported by Forbush (1946). GLEs are large SEP events that are observed by ground-based experiments such as neutron monitors (NMs). These detectors measure

✉ P. Kühl
    kuehl@physik.uni-kiel.de

[1] Institute for Experimental and Applied Physics, University Kiel, 24118 Kiel, Germany

🙂 Springer

secondary particles that are produced when ions with energies above several hundred of MeVs create a nuclear cascade in the Earth's atmosphere. Since 1942, 71 GLEs have been reported (see *e.g.* https://gle.oulu.fi/); the largest measured increase above the pre-event background of about 4500 % was observed during GLE 5 on 23 February 1956 (Reames, 2013).

In order to fully understand the physics behind the particles resulting in GLEs, the chain of acceleration in the corona, the injection and transport in interplanetary space, and the propagation through the Earth's magnetosphere and atmosphere have to be understood. To this aim, Mishev, Usoskin, and Kovaltsov (2013) calculated the atmospheric yield function that describes the relationship between the intensity of protons and α-particles near Earth and the neutron monitor count rate, showing significant values for proton energies above 700 MeV. In agreement to these findings, investigations by Gopalswamy and Mäkelä (2014) using the *Geostationary Operational Environmental Satellite* (GOES) measurements of protons with energies above 700 MeV showed a good correlation between the occurrence of above 700 MeV SEPs and GLEs during Solar Cycles 23 and 24. However, in an extended study, Thakur *et al.* (2016) have reported two exceptions out of the 16 GLEs observed during Solar Cycles 23 and 24. The event of 6 May 1998 caused a GLE, but did not cause an increase in measurements above 700 MeV in GOES, and the 8 November 2000 event caused an increase of above 100 % with respect to the pre-event background in the GOES channel, but no increase in the neutron monitor network.

This dilemma, when a solar energetic particle event with a proton intensity increase at energies above 700 MeV observed in the near-Earth environment is recorded as a GLE and *vice versa*, also depends on the measurement capabilities of the available instruments. While NMs are a valuable tool to investigate GLEs, they have several limitations that are due to the indirect nature of detection. By measuring the count rate of secondary particles at the ground, a count which is created by interactions of high-energy particles with the atmosphere, NMs do not provide any direct information regarding the interplanetary spectrum of particles. In addition, the Earth's magnetosphere and hence the resulting geomagnetic cutoff rigidity (Lockwood and Debrunner, 1999) can vary over time, further increasing the uncertainties in the analysis of NM data. In addition to simulations of these magnetospheric and atmospheric effects, knowledge of the energy spectrum outside of the magnetosphere is therefore required. We recently showed that the *Electron Proton Helium Instrument* (EPHIN) is capable of measuring proton energy spectra up to 1 GeV (Kühl *et al.*, 2015a,b; Kühl, Gómez-Herrero, and Heber, 2016; Heber *et al.*, 2015), providing the necessary data for this type of investigation.

In this article, this new data are used to identify SEP events with protons above 500 MeV during the time period of 1995 to 2015. A detailed comparison with other event lists is carried out. Furthermore, a statistical analysis of the events based on their spectral properties and on the neutron monitor count rate increase for events resulting in GLEs is presented.

The article is structured as follows. In Section 2 the instrumentation and data are described. In Section 3 we identify events and compile an event list. Finally, in Section 4, we present a statistical analysis of the event list by analyzing the proton spectra, while in Section 5 we summarize our results.

2. Instrumentation and Data

2.1. Validation of High-Energy Proton Channels During Different Event Phases

The EPHIN instrument (Müller-Mellin *et al.*, 1995) onboard the *Solar and Heliospheric Observatory* (SOHO) consists of a stack of six silicon semiconductors labeled A to F that
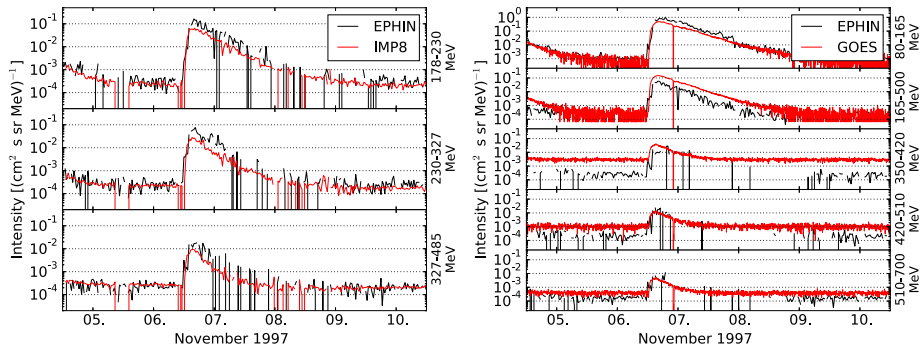
Figure 1 Proton intensities of the November 1997 GLE measured in different energy channels by IMP-8/GME (left panels, red curves) and GOES-9/EPS and GOES-9/HEPAD (right panels, red curves). For comparison, intensities for the same energy channels derived in this study from SOHO/EPHIN data (black curves) are presented.

are surrounded by an anticoincidence detector. The nominal energy range, between 5 and 50 MeV for protons, was extended to energies from 100 MeV to above 1 GeV with a method first presented by Kühl *et al.* (2015a). The method is based on particles that penetrate the entire detector stack, depositing only a fraction of their kinetic energy in the instrument. For these penetrating particles, the energy deposition in detectors C and D is taken as a measurement of the energy losses of these particles. It has been shown that for energy losses in a certain range, a reliable particle identification is possible for the penetrating particles. The energy losses can then be converted back into total kinetic energy with an uncertainty between 10 % (at 100 MeV) and 20 % (at 1 GeV, *cf.* Figure 9 in Kühl *et al.*, 2015a). For a more detailed description of the method, we refer to Kühl *et al.* (2015a) and Kühl, Gómez-Herrero, and Heber (2016).

The method has been successfully validated for the solar energetic particle events on 17 May 2012 and 6 January 2014 (Kühl *et al.*, 2015a). Kühl, Gómez-Herrero, and Heber (2016) have proven that the method is also applicable in the absence of solar events to derive galactic cosmic-ray (GCR) spectra from 250 MeV up to 1.6 GeV.

In this article, the method is used to identify solar energetic particle events with protons accelerated to at least 500 MeV. To apply this method to the entire SEP event, a further validation of the method during the entire solar event (including the rising and declining phases) is necessary since Kühl *et al.* (2015a) have only calculated event spectra for certain time periods. Since the method individually reconstructs the energy for every detected particle, it provides the opportunity of defining any arbitrary energy channel between ≈ 100 MeV up to above 1 GeV. Hence, intercalibration and comparison with other missions can be achieved rather easily.

For this purpose, Figure 1 shows the intensity of different energy channels during the 6 November 1997 SEP event (GLE 55) measured by the *Goddard Medium Energy Experiment* (GME: McGuire, von Rosenvinge, and McDonald, 1986) onboard the *Interplanetary Monitoring Platform 8* (IMP-8) in the left panels and by the *Energetic Particle Sensor* (EPS: Onsager *et al.*, 1996) and the *High Energy Proton and Alpha Detector* (HEPAD: Hanser, 2011) onboard GOES-9 in the right panels. In addition, the measured SOHO/EPHIN intensities in the same energy range are shown (black curves in both panels). The figure clearly shows that all three instruments measure the SEP event and that the intensity *vs.* time profiles are in agreement within a factor of two.
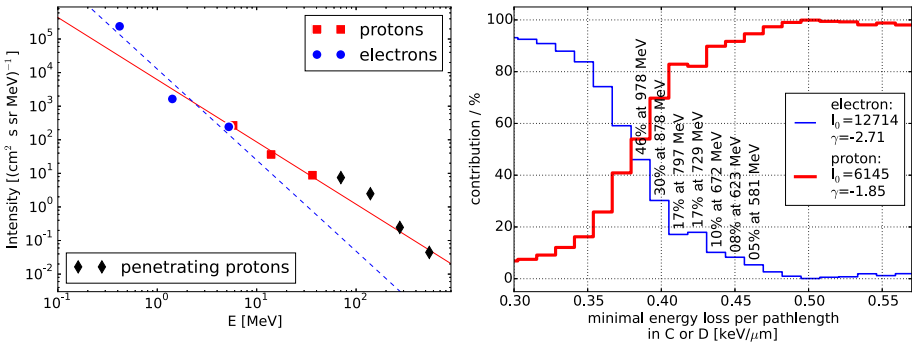
Figure 2 Left panel: proton (red squares) and electron (blue circles) spectra from the nominal data products and power law fits (lines) for GLE 69 on 20 January 2005 from 09:00 – 11:00 UT. For the same time period, the spectra of protons penetrating the instrument was also derived (black diamonds). Right panel: simulation results showing the contribution of protons and electrons for different energy losses based on the extrapolated spectra. The extrapolation was made with a power-law fit for both particle spectra with the fit results given in the legend. For some exemplary energy losses, the electron contribution and the proton energy related to that energy loss are shown by the text included in the vertical direction.

However, EPHIN systematically measures higher intensities around the maximum and in the decay phase of the event when compared to the IMP-8 instrument in all three channels. In contrast, the intensities are in agreement before and after the event. Hence we attribute the differences during the event to the so-called ring switching (for details see Müller-Mellin *et al.*, 1995).

It is important to note that the pre-event background measured by GOES is an order of magnitude higher than the backgrounds given by EPHIN and the IMP-8 instrument, as has been described by Sandberg *et al.* (2014). Furthermore, the 30-minute averaged data from SOHO/EPHIN have statistical limitations, especially in the decay phase of the event.

2.2. Electron Contamination of the High-Energy Proton Measurements

Kühl *et al.* (2015a) have mentioned a possible influence of electron fluxes above 10 MeV on the high-energy proton data during solar events, but this issue has not been quantified yet. Heber *et al.* (2015) showed that there are discrepancies in the derived proton spectrum during GLE 69 between SOHO and neutron monitors above 700 MeV, while GOES and SOHO agree with each other at lower energies. The increased flux above 700 MeV is believed to be caused by electrons above 10 MeV that are associated with the same SEP event that causes similar energy losses in the detector compared to those of high-energy protons. Therefore, the influence of electrons on the derived proton flux above 700 MeV has to be taken into account, and a study of this effect is necessary before a detailed analysis of the spectral properties can be performed.

For this purpose, Figure 2 (left panel) presents electron (blue circles) and proton (red squares) spectra based on the nominal data products from the EPHIN instrument during the GLE 69 on 20 January 2005 from 09:00 – 11:00 UT. The event has one of the highest electron contributions of the events investigated in this study and can therefore be considered as the worst-case scenario. The spectra were fitted with a power law and have been extrapolated to higher energies. We note that although the derived proton spectra based on the penetrating particles (black diamonds) are in agreement with the power law fitted to the proton spectrum

below 50 MeV, a softening in the proton spectrum at higher energies (*e.g.* a double power law) would increase the electron contribution. Using the fitted spectra as input for a Geometry and Tracking 4 (GEANT4) Monte Carlo simulation (GEANT4 collaboration, 2006) of the instrument, we derived the contribution of both protons and electrons to energy losses in the C and D detectors. As a result, Figure 2 (right) shows the contribution of electrons (blue) and protons (red) dependent on the energy loss. For some illustrative energy losses, the electron contribution and the proton energy related to that energy loss are shown by the text included in the vertical direction. The figure shows that the electron contribution to the high-energy proton spectra is: 1) negligible below ≈ 500 MeV, 2) lower than 20 % in the energy range from 500 to 800 MeV, and 3) very strong above 800 MeV. Hence, proton intensities above 800 MeV should be considered as upper limits during solar events.

## 3. Identification Method of > 500 MeV Proton Events

3.1. Event Detection

In order to identify SEPs with protons accelerated to energies above 500 MeV, a histogram of hourly intensities in a defined $500 - 700$ MeV range from 1995 to 2015 is presented in Figure 3. The histogram indicates that most of the time, the measured intensity is in the range of $0.7 - 4 \cdot 10^{-4}$ $(\text{cm}^2\,\text{s}\,\text{sr}\,\text{MeV})^{-1}$. In agreement with Kühl, Gómez-Herrero, and Heber (2016), these intensities correspond to the GCR background. The variation of the peak position over different years as indicated by annual histograms can be explained by solar modulation (Heber and Potgieter, 2006; Heber, Fichtner, and Scherer, 2006). While intensities below this main population correspond to either GCR depressions during the passages of interplanetary coronal mass ejections (Forbush decreases, Cane, 2000) or instrumental effects such as a high dead time of the electronics, higher intensities are related to SEPs.

In this study, events have been identified by requiring that at least two hourly averaged intensities in a six-hour interval are above a threshold of $4 \cdot 10^{-4}$ $(\text{cm}^2\,\text{s}\,\text{sr}\,\text{MeV})^{-1}$. Using this identification technique, we identified 42 solar particle events in the time between the start of the mission (December 1995) and 1 October 2015. It has to be noted that communication with SOHO was lost for several months during 1998 and, hence, no EPHIN data are available for this time period.

3.2. The Event List

Figure 4 presents the time profile of the proton intensity in the energy range from 500 to 700 MeV over the past 20 years. In agreement with Figure 3, the variation of the GCR

Figure 3 Histograms of the hourly proton intensities in the energy range from 500 to 700 MeV based on SOHO/EPHIN data. Shown are a histogram of the entire mission, as well as three annual histograms, as indicated in the inset.
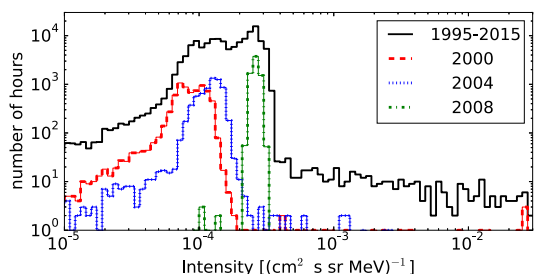
Figure 4 Time profile of the proton intensity in the energy range of 500 to 700 MeV averaged over six hours for the past 20 years. The dashed vertical lines and the arrows indicate the dates of the SEP events found in this study.
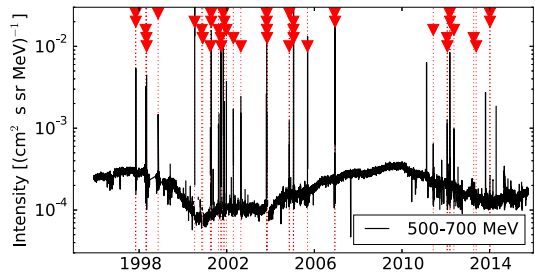
background intensity lies between 0.7 and $4 \cdot 10^{-4}$ $(\mathrm{cm^2\,s\,sr\,MeV})^{-1}$ over Solar Cycles 23 and 24. The dates of the events identified in this study are marked as red triangles. We note that some intensity increases shown in the figure were not selected as events since they were caused by photons from the flare (in the range of the extreme-ultraviolet to hard X-rays) depositing energy in the detector stack. Since these photon peaks are typically short lived, they do not increase the intensity over two hours and are therefore not identified by the algorithm. Of the 42 events, 32 events occurred during Solar Cycle 23 and only ten in Solar Cycle 24. As expected, the occurrence of the solar events is clearly more likely during solar maxima (around 2002 and 2014, Nymmik, 1999).

The dates and times when the events passed the threshold are listed in columns two and three of Table 1. We note that these numbers mark the time when the event was identified by the algorithm, and they are not to be confused with onset times. The onset times are derived in Section 4.1. Columns five to eight give the corresponding events from other studies, namely GLEs (taken from http://gle.oulu.fi/), SEPServer (Vainio *et al.*, 2013), GOES (major sep list, http://cdaw.gsfc.nasa.gov/CME_list/sepe/), and Gopalswamy *et al.* (2015), respectively. The exact times of the GLEs were taken from the Neutron Monitor Database (NMDB, http://www.nmdb.eu/nest/gle_list.php). GLE 68 is listed at 00:00 UT by the NMDB, while Cliver (2006) related this GLE to a flare peaking at 09:52 UT. Hence, for this event, the time from Cliver (2006) was adopted.

Events 35, 36, and 41 are listed as sub-GLEs in the Oulu GLE database (https://gle.oulu.fi/), and event 42 was suggested to be a GLE by Thakur *et al.* (2014). However, they are not officially confirmed to be GLEs, and therefore they are not marked as GLEs in our table.

The table clearly shows that the 42 events include all GLEs during the SOHO age (GLE 55 to GLE 72) with the exception of GLE 58, during which SOHO had a data gap. Since GLEs are known to be caused by events during which particles are accelerated to above 500 MeV (Cliver *et al.*, 1983; Plainaki *et al.*, 2009; Shen *et al.*, 2013), this is a validation of the event identification method.

Because the SEPServer list is based on data from 1996 to 2010, it also includes the majority of the events found in this study. The GOES list features every single event found in this study. Gopalswamy *et al.* (2015) have derived a list of 37 large solar events for Solar Cycle 24 that occurred until the end of 2014. Only ten of these events were detected by our method, suggesting that the other 27 events did not accelerate protons to energies above 500 MeV. In their analysis, Gopalswamy *et al.* (2015) identified eight GLE candidates from their list. Of these eight events, only three are found to have increased fluxes above 500 MeV based on this study (events 33, 38, and 40).

Table 1 Event list compiled in this article. The columns represent the event number (column 1), the date (column 2), and the time (column 3) when the intensity threshold was surpassed, the onset time (column 4), corresponding event numbers of the GLE (http://gle.oulu.fi/, Sub-GLE are also marked) (column 5), SEPServer (Vainio *et al.*, 2013) (column 6), GOES (http://cdaw.gsfc.nasa.gov/CME_list/sepe/) (column 7), and Gopalswamy *et al.* (2015) (column 8) event lists. A *p* in the onset time indicates that the time corresponds to the day before the date given in column 1. For details see text.

No.	Date	Time	Onset	GLE No.	SEPS	GOES	Gopalswamy
01	04-11-1997	15:00	06:00	–	2	1	–
02	06-11-1997	13:00	12:45	55	3	2	–
03	20-04-1998	20:00	–	–	6	3	–
04	02-05-1998	18:00	15:00	56	7	4	–
05	06-05-1998	13:00	08:30	57	8	5	–
06	14-11-1998	09:00	06:15	–	12	11	–
07	14-07-2000	12:00	10:30	59	32	21	–
08	09-11-2000	01:00	23:30p	–	38	28	–
09	26-11-2000	18:00	–	–	–	30	–
10	03-04-2001	04:00	01:00	–	45	33	–
11	15-04-2001	16:00	15:00	60	49	36	–
12	18-04-2001	04:00	02:45	61	50	37	–
13	16-08-2001	03:00	00:30	–	–	42	–
14	24-09-2001	23:00	14:00	–	58	44	–
15	01-10-2001	22:00	–	–	59	45	–
16	04-11-2001	17:00	16:30	62	63	48	–
17	23-11-2001	05:00	21:00p	–	64	51	–
18	26-12-2001	07:00	06:30	63	65	52	–
19	21-04-2002	06:00	02:00	–	72	63	–
20	24-08-2002	04:00	02:15	64	80	71	–
21	28-10-2003	13:00	14:00	65	88	78	–
22	29-10-2003	22:00	21:15	66	–	79	–
23	02-11-2003	20:00	17:15	67	90	81	–
24	05-11-2003	06:00	02:00	–	–	82	–
25	07-11-2004	21:00	15:45	–	97	90	–
26	10-11-2004	11:00	03:15	–	99	92	–
27	16-01-2005	14:00	–	–	101	93	–
28	17-01-2005	16:00	13:45	68	–	94	–
29	20-01-2005	09:00	06:45	69	–	95	–
30	08-09-2005	20:00	–	–	–	102	–
31	06-12-2006	23:00	–	–	–	104	–
32	13-12-2006	04:00	03:00	70	112	105	–
33	07-06-2011	09:00	07:15	–	–	110	4
34	23-01-2012	12:00	05:30	–	–	115	9
35	28-01-2012	04:00	18:30p	–	–	116	10
36	07-03-2012	04:00	–	–	–	117	11
37	13-03-2012	19:00	17:45	–	–	118	12
38	17-05-2012	03:00	01:45	71	–	119	13
39	11-04-2013	12:00	07:45	–	–	131	25
40	22-05-2013	20:00	14:00	–	–	133	27
41	06-01-2014	10:00	–	–	–	137	31
42	08-01-2014	00:00	21:00p	–	–	138	32

Figure 5 Proton spectrum with power-law fit for event 2 (GLE 55) from 13:15 to 15:15 UT. Note that only energies below 800 MeV have been used for the fit because of possible electron contamination at higher energies.
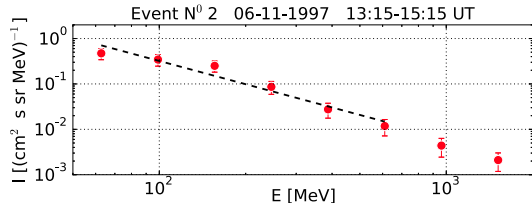
Table 2 Energy bins used for the spectra.

Lower bin edge [MeV]	49	78	124	195	308	486	766	1207
Upper bin edge [MeV]	78	124	195	308	486	766	1207	1903
Geometric mean [MeV]	62	98	155	245	387	610	962	1516

4. Statistical Event Analysis

4.1. Onset Times

For a study of the spectral properties of the events, we took into account only those events for which an onset time based on a 100 to 1000 MeV proton channel could be derived. The chosen broader energy interval in comparison to the 500 to 700 MeV interval allows us to determine the onset with a time resolution of 15 minutes. For 34 of the 42 events, it was possible to derive the onset time by requiring an intensity increase above a threshold defined as the average intensity during the previous six hours plus three times the standard deviation of that time interval. These 34 events include all GLEs and sub-GLEs except for event 41, since EPHIN had a data gap during the early stage of the event (Kühl *et al.*, 2015a). Hence, no onset could be determined for this event, and it is excluded from the following analysis. All determined onset times are listed in column four of Table 1.

4.2. Event Spectra

Since the statistics of EPHIN data for event 25 are limited, it was excluded from the following study, although an onset time was derived. For the remaining 33 events, the high-energy proton spectrum was calculated in a time interval of two hours, starting 30 minutes after the onset. The time lag of 30 minutes is necessary to reflect the different travel times of 100 MeV and 1000 MeV protons. While the latter can reach the spacecraft after about ten minutes (depending on the length of the Parker spiral and the diffusion in the interplanetary medium), the 100 MeV protons can be delayed by up to half an hour because of their lower velocity. The interval length of two hours was selected for statistical reasons. As an example, Figure 5 shows the derived spectrum for event 2 (GLE 55). In the figure, the geometric mean of the energy range is shown. The exact energy bins are given in Table 2.

Mewaldt *et al.* (2012) have shown that the proton spectra of GLE events can be reproduced by a double-power law (described by Band *et al.*, 1993) with a spectral break at several MeV. Since we only analyze energies above 100 MeV, a single power-law function

$$I(E) = I_0 \cdot (E/E_0)^\gamma, \tag{1}$$

where the intensities $I(E)$ and I_0 are measured in $[(cm^2 \, s \, sr \, MeV)^{-1}]$ and the energies E, E_0 in [MeV], was fitted for every single event. Based on the approximation of the electron

Table 3 Results of the power law fit to the proton spectra. The columns represent the event number (*cf.* Table 1, column 1), the fitted spectral indices [γ] (column 2), and intensities at 500 MeV [I_{500}] (in units of [$(cm^2 \, s \, sr \, MeV)^{-1}$], column 3) of the events. Since the fit was performed as a linear regression between the logarithm of the energy and the logarithm of the intensity, the goodness of the fits is represented by the adjusted coefficient of determination [R^2] (column 4). For details see text.

No.	γ	[I_{500}]	R^2	No.	γ	[I_{500}]	R^2
01	-2.20 ± 0.16	(8.77 ± 1.00) e–4	0.97	21	-3.15 ± 0.25	(2.07 ± 0.15) e–2	0.97
02	-1.70 ± 0.24	(2.08 ± 0.33) e–2	0.95	22	-2.49 ± 0.11	(3.70 ± 0.15) e–2	1.00
04	-2.12 ± 0.15	(2.31 ± 0.21) e–3	0.96	23	-2.70 ± 0.22	(1.50 ± 0.11) e–2	0.98
05	-2.84 ± 0.26	(1.15 ± 0.12) e–3	0.93	24	-2.67 ± 0.17	(3.45 ± 0.30) e–4	0.98
06	-2.44 ± 0.24	(1.52 ± 0.18) e–3	0.91	26	-1.51 ± 0.11	(9.92 ± 1.94) e–4	0.97
07	-2.24 ± 0.15	(1.74 ± 0.11) e–1	0.97	28	-3.20 ± 0.08	(6.12 ± 0.14) e–3	0.93
08	-2.78 ± 0.31	(1.32 ± 0.14) e–1	0.97	29	-2.12 ± 0.13	(2.53 ± 0.14) e–1	0.99
10	-3.24 ± 0.12	(5.59 ± 0.23) e–4	0.98	32	-1.95 ± 0.15	(3.56 ± 0.26) e–2	0.98
11	-2.13 ± 0.03	(7.77 ± 0.10) e–2	0.99	33	-1.83 ± 0.31	(9.85 ± 3.15) e–4	0.85
12	-2.01 ± 0.12	(3.79 ± 0.31) e–3	0.97	34	-3.78 ± 0.40	(2.45 ± 0.27) e–4	0.78
13	-2.57 ± 0.09	(2.38 ± 0.10) e–3	0.99	35	-2.22 ± 0.24	(1.65 ± 0.25) e–3	0.93
14	-3.30 ± 0.33	(4.39 ± 0.47) e–4	0.93	37	-2.75 ± 0.25	(1.84 ± 0.18) e–3	0.94
16	-2.90 ± 0.20	(1.06 ± 0.07) e–2	0.98	38	-1.87 ± 0.17	(4.47 ± 0.57) e–3	0.97
17	-2.22 ± 0.05	(5.55 ± 0.21) e–4	1.00	39	-2.19 ± 0.09	(3.40 ± 0.26) e–4	0.99
18	-3.21 ± 0.07	(5.39 ± 0.11) e–3	0.99	40	-2.93 ± 0.19	(5.55 ± 0.43) e–4	0.92
19	-3.84 ± 0.10	(2.35 ± 0.06) e–3	0.97	42	-3.60 ± 0.03	(4.93 ± 0.04) e–4	1.00
20	-2.58 ± 0.08	(4.41 ± 0.15) e–3	1.00				

contribution described above (*cf.* Figure 2), only energies below 800 MeV were taken into account for the fit because of possible electron contamination at higher energies. As an example, the fit for event 2 is shown in Figure 5.

Table 3 presents the spectral indices [γ] and intensities at 500 MeV [I_{500}] resulting from the fits of the 33 events. The fit was performed as a linear regression between the logarithm of the energy and the logarithm of the intensity. Hence, the goodness of the fits can be represented by the adjusted determination coefficient [R^2], which is also given in Table 3.

4.3. Statistical Analysis of > 500 MeV Proton Events

In Figure 6 the spectral index of the analyzed events is shown as a function of the proton intensity at 500 MeV derived from the proton spectrum fits. GLEs are shown as red squares, the remaining events are plotted as black circles. The numbers in the symbols correspond to those in Tables 1 and 3. The dark gray and light gray shaded areas correspond to the varying GCR background level at 500 MeV during solar maximum and solar minimum, respectively (*cf.* Figure 3). At the top and at the right-hand side of the figure, histograms of both quantities are also shown individually.

The fit results of events 24, 34, and 39 show that the proton intensity at the energy of 500 MeV is slightly lower than the threshold used for the event identification based on the 500 – 700 MeV channel. This can be explained by statistical errors of the channel intensity and the fit results. However, it should be noted that these events occurred during solar maximum and hence might still have caused an increase above the GCR background.

Figure 6 Bottom left: spectral index [γ] as a function of intensity at 500 MeV derived from the proton spectrum fits. GLEs are marked as red squares, other events as black circles. All numbers correspond to those in Tables 1 and 3. The gray shaded areas (see text) mark the GCR background level in terms of intensity. Top and right: histograms of the intensity at 500 MeV and the spectral index [γ], respectively. The solid red line corresponds to GLEs. Other events are represented by a dashed black line.
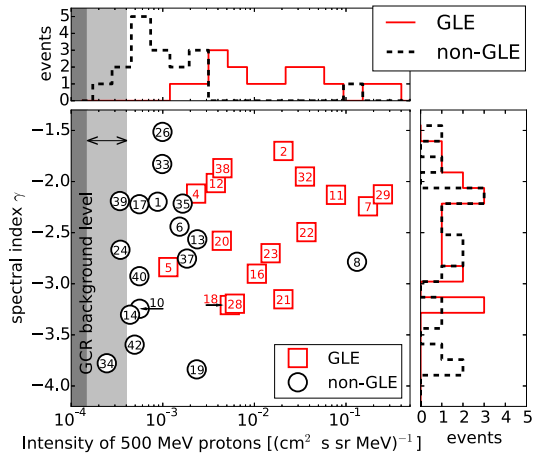

Event 08 shows a much higher intensity than and a similar spectral index as several GLEs, but still shows no increases in the neutron monitor count rates, which is in agreement with findings of Thakur *et al.* (2016). Hence, this event is of special interest in terms of understanding which physical processes determine whether an SEP event with a certain spectral shape is observed by the neutron monitor network. Therefore, an extensive study using not only the spectral data at high energies, but also simulations of the asymptotic viewing directions of neutron monitors is in preparation.

The majority of the GLEs feature spectral indices that are uniformly distributed between -2 and -3, which is in good agreement with the results of Mewaldt *et al.* (2012). The spectral indices of events not related to GLEs are also uniformly distributed, but in a wider range between -2 and -4. The spectral index of event 20 ($\gamma = -2.58$) is identical with the findings of Tylka *et al.* (2006).

However, the intensity of 500 MeV protons is typically higher during GLE-related events than during events without GLEs. Furthermore, this intensity is above $2 \cdot 10^{-3}$ $(cm^2\,s\,sr\,MeV)^{-1}$ for all GLEs (except for event 5), which is consistent with the results of Nitta *et al.* (2012). In their study, these authors showed that the GOES/HEPAD P9 channel ($420-510$ MeV) typically exceeds $2 \cdot 10^{-3}$ $(cm^2\,s\,sr\,MeV)^{-1}$ during GLEs with only GLE 57 and GLE 68, corresponding to events 05 and 28 in our list, having lower fluxes. Thakur *et al.* (2016) also found GLE 57 to be an especially small event. While the results of this work do confirm the results of previous studies regarding the low intensity of GLE 57, the intensity of GLE 68 is found to be higher than the results of Nitta *et al.* (2012). However, in their study, Nitta *et al.* (2012) noted that the onset determination and hence the analysis of this particular event is troublesome.

The five GLEs with the highest flux in our analysis (events 29, 07, 11, 22, and 32, corresponding to GLEs 69, 59, 60, 66, and 70) are also considered to be among the largest GLEs in the SOHO era (*cf.* Table 1 in McCracken, Moraal, and Shea, 2012). The relative increases in neutron monitor count rate for GLEs given by McCracken, Moraal, and Shea (2012) are shown as a function of the intensity at 500 MeV derived in this study in Figure 7. Some GLEs from Table 1 are not shown here, as they have not been investigated by Mc-Cracken, Moraal, and Shea (2012). The figure indicates a correlation between the intensity at 500 MeV and the relative increase in NM count rate, with the exception of events whose intensities are below 10^{-2} $(cm^2\,s\,sr\,MeV)^{-1}$ (events 12, 18, and 38) and event 29, which has a significantly higher increase in NM count rate than the measured intensity at 500 MeV.

Figure 7 Relative increase of
the neutron monitor count rate as
a function of intensity at
500 MeV based on the fit. The
increase in the NM count rates is
taken from McCracken, Moraal,
and Shea (2012). The numbers
correspond to Tables 1 and 3.
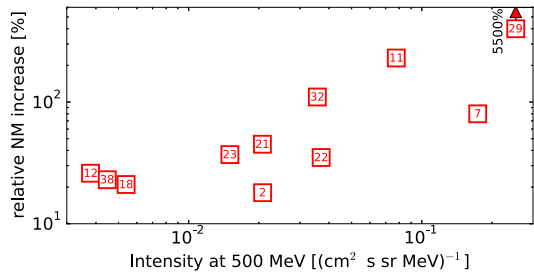
Furthermore, it has to be noted that the scattering of the relative NM count rate increase
for a given intensity at 500 MeV is rather high. The reasons for these deviations remain
unclear, especially since the spectral shape of the events (*e.g.* the fitted γ) are rather similar
for most of them (*cf.* Figure 6). Possible explanations are the asymptotic viewing direction
of each neutron monitor (McCracken and Freon, 1962; Smart, Shea, and Flückiger, 2000)
or changes in the cutoff rigidities that are due to geomagnetic disturbances during the SEP
events (Danilova, 1999), which may differ from event to event.

5. Summary

We investigate SEP events with protons with energies above 500 MeV based on the extended
measurement range of SOHO/EPHIN described by Kühl *et al.* (2015a) and Kühl, Gómez-
Herrero, and Heber (2016).

   We show that the new and unique data product is valid during any stage of the solar event
(*e.g.* onset, maximum, and decay phase) by comparison with results from IMP8 and GOES.
Furthermore, additional simulations of the instrument show that the electron contribution to
the high-energy proton data is: 1) negligible below 500 MeV, 2) lower than 20 % between
500 and 800 MeV, and 3) seriously uncertain above 800 MeV.

   Based on the energy interval from 500 to 700 MeV, 42 SEP events with protons acceler-
ated to above 500 MeV have been identified during the last 20 years of the SOHO mission.
The compiled event list (see Table 1) was compared to various other event lists, including
the GLE list.

   For events with clear onset times, the proton intensity spectra were derived in a time
interval of two hours, starting 30 minutes after the onset time. The spectral indices [γ]
derived from the power-law fit in the energy range below 800 MeV and the intensity at
500 MeV of the events were compared (see Figure 6 and Table 3).

   Based on this comparison, various results from the literature such as typical intensity
increases above $2 \cdot 10^{-3}$ $(\text{cm}^2\,\text{s}\,\text{sr}\,\text{MeV})^{-1}$ at 500 MeV (Nitta *et al.*, 2012) were validated.
Furthermore, certain non-GLE and GLE events with surprisingly high and low intensity,
respectively, were found, in agreement with Thakur *et al.* (2016).

   Comparing the derived intensities at 500 MeV with the relative increase of the neutron
monitor count rates during GLEs (McCracken, Moraal, and Shea, 2012), a clear correlation
was found, with the exception of events with a very low intensity at 500 MeV and GLE 69,
which shows a particularly strong increase in the neutron monitor count rate.

Disclosure of Potential Conflicts of Interest   The authors declare that they have no conflicts of interest.

References

Band, D., Matteson, J., Ford, L., Schaefer, B., Palmer, D., Teegarden, B., Cline, T., Briggs, M., Paciesas, W., Pendleton, G., Fishman, G., Kouveliotou, C., Meegan, C., Wilson, R., Lestrade, P.: 1993, BATSE observations of gamma-ray burst spectra. I – Spectral diversity. *Astrophys. J.* **413**, 281. DOI.

Cane, H.V.: 2000, Coronal mass ejections and Forbush decreases. *Space Sci. Rev.* **93**, 55. DOI.

Cliver, E.W.: 2006, The unusual relativistic solar proton events of 1979 August 21 and 1981 May 10. *Astrophys. J.* **639**, 1206. DOI.

Cliver, E.W., Kahler, S.W., Cane, H.V., Koomen, M.J., Michels, D.J., Howard, R.A., Sheeley, N.R. Jr.: 1983, The GLE-associated flare of 21 August, 1979. *Solar Phys.* **89**, 181. DOI. ADS.

Danilova, O.: 1999, The GLE of May 2, 1998: An effect of disturbed magnetosphere on solar cosmic rays. In: *Int. Cosmic Ray Conf.* **6**, 399. ADS.

Forbush, S.E.: 1946, Three unusual cosmic-ray increases possibly due to charged particles from the Sun. *Phys. Rev.* **70**, 771. DOI.

GEANT4 collaboration: 2006, An object-oriented toolkit for simulation in hep. CERN-LHCC 98-44. See also http://geant4.cern.ch/.

Gopalswamy, N., Mäkelä, P.: 2014, Latitudinal connectivity of ground level enhancement events. In: Hu, Q., Zank, G.P. (eds.) *Outstanding Problems in Heliophysics: From Coronal Heating to the Edge of the Heliosphere*, *Astron. Soc. Pacific Conf. Ser.* **484**, 63. ADS.

Gopalswamy, N., Mäkelä, P., Yashiro, S., Xie, H., Akiyama, S., Thakur, N.: 2015, High-energy solar particle events in cycle 24. *J. Phys. Conf. Ser.* **642**(1), 012012. DOI.

Hanser, F.A.: 2011, EPS/HEPAD calibration and data handbook. Tech. rep. goesn-eng-048d. Available at www.ngdc.noaa.gov/stp/satellite/goes/documentation.html. DOI.

Heber, B., Fichtner, H., Scherer, K.: 2006, Solar and heliospheric modulation of galactic cosmic rays. *Space Sci. Rev.* **125**, 81. DOI. ADS.

Heber, B., Potgieter, M.S.: 2006, Cosmic rays at high heliolatitudes. *Space Sci. Rev.* **127**, 117. DOI. ADS.

Heber, B., Dresing, N., Herbst, K., Klassen, A., Kühl, P., Gómez-Herrero, R.: 2015, Proton energy spectra during ground level enhancements as measured by EPHIN aboard SOHO. In: *Proc. Science ICRC 2015*.

Kühl, P., Gómez-Herrero, R., Heber, B.: 2016, Annual cosmic ray spectra from 250 MeV up to 1.6 GeV from 1995 – 2014 measured with the electron proton helium instrument onboard SOHO. *Solar Phys.* **291**, 965. DOI.

Kühl, P., Banjac, S., Dresing, N., Gómez-Herrero, R., Heber, B., Klassen, A., *et al.*: 2015a, Proton intensity spectra during the solar energetic particle events of May 17, 2012 and January 6, 2014. *Astron. Astrophys.* **576**, A120. DOI. ADS.

Kühl, P., Dresing, N., Gieseler, J., Heber, B., Klassen, A.: 2015b, Galactic cosmic ray spectra during solar cycle 23 and 24 – Measurement capabilities of the electron proton helium instrument. In: *Proc. Science ICRC 2015*.

Lockwood, J.A., Debrunner, H.: 1999, Solar flare particle measurements with neutron monitors. *Space Sci. Rev.* **88**, 483. DOI. ADS.

McCracken, K.G., Freon, A.: 1962, Asymptotic directions and cut-off rigidities in the geomagnetic field. *J. Phys. Soc. Japan* **17**, AII, 455. ADS.

McCracken, K.G., Moraal, H., Shea, M.A.: 2012, The high-energy impulsive ground-level enhancement. *Astrophys. J.* **761**, 101. DOI.

McGuire, R.E., von Rosenvinge, T.T. McDonald, F.B.: 1986, The composition of solar energetic particles. *Astrophys. J.* **301**, 938. DOI.

Mewaldt, R.A., Looper, M.D., Cohen, C.M.S., Haggerty, D.K., Labrador, A.W., Leske, R.A., Mason, G.M., Mazur, J.E., von Rosenvinge, T.T.: 2012, Energy spectra, composition, and other properties of ground-level events during solar cycle 23. *Space Sci. Rev.* **171**, 97. DOI.

Mishev, A.L., Usoskin, I.G., Kovaltsov, G.A.: 2013, Neutron monitor yield function: New improved computations. *J. Geophys. Res.* **118**, 2783. DOI. ADS.

Müller-Mellin, R., Kunow, H., Fleißner, V., Pehlke, E., Rode, E., Röschmann, N., *et al.*: 1995, Costep – Comprehensive suprathermal and energetic particle analyser. *Solar Phys.* **162**, 483.

Nitta, N.V., Liu, Y., DeRosa, M.L., Nightingale, R.W.: 2012, What are special about ground-level events? Flares, CMEs, active regions and magnetic field connection. *Space Sci. Rev.* **171**, 61. DOI. ADS.

Nymmik, R.: 1999, Relationships among solar activity SEP occurrence frequency, and solar energetic particle event distribution function. In: *Int. Cosmic Ray Conf.*, **6**, 280. ADS.

Onsager, T., Grubb, R., Kunches, J., Matheson, L., Speich, D., Zwickl, R.W., Sauer, H.: 1996, Operational uses of the GOES energetic particle detectors. In: Washwell, E.R. (ed.) *GOES-8 and Beyond*, *Proc. SPIE* **2812**, 281. DOI.

Plainaki, C., Mavromichalaki, H., Belov, A., Eroshenko, E., Yanke, V.: 2009, Modeling the solar cosmic ray event of 13 December 2006 using ground level neutron monitor data. *Adv. Space Res.* **43**, 474. DOI. ADS.

Reames, D.V.: 2013, The two sources of solar energetic particles. *Space Sci. Rev.* **175**, 53. DOI. ADS.

Sandberg, I., Jiggens, P., Heynderickx, D., Daglis, I.A.: 2014, Cross calibration of NOAA GOES solar proton detectors using corrected NASA IMP-8/GME data. *Geophys. Res. Lett.* **41**, 4435. DOI. ADS.

Shen, C., Li, G., Kong, X., Hu, J., Sun, X.D., Ding, L., Chen, Y., Wang, Y., Xia, L.: 2013, Compound twin coronal mass ejections in the 2012 May 17 GLE event. *Astrophys. J.* **763**, 114. DOI. ADS.

Smart, D.F., Shea, M.A., Flückiger, E.O.: 2000, Magnetospheric models and trajectory computations. *Space Sci. Rev.* **93**, 305. DOI. ADS.

Thakur, N., Gopalswamy, N., Xie, H., Mäkelä, P., Yashiro, S., Akiyama, S., Davila, J.M.: 2014, Ground level enhancement in the 2014 January 6 solar energetic particle event. *Astrophys. J. Lett.* **790**, L13. DOI. ADS.

Thakur, N., Gopalswamy, N., Mäkelä, P., Akiyama, S., Yashiro, S., Xie, H.: 2016, Two exceptions in the large SEP events of solar cycles 23 and 24. *Solar Phys.* **291**, 513. DOI.

Tylka, A.J., Cohen, C.M.S., Dietrich, W.F., Lee, M.A., Maclennan, C.G., Mewaldt, R.A., Ng, C.K., Reames, D.V.: 2006, A comparative study of ion characteristics in the large gradual solar energetic particle events of 2002 April 21 and 2002 August 24. *Astrophys. J. Suppl.* **164**, 536. DOI. ADS.

Vainio, R., Valtonen, E., Heber, B., Malandraki, O.E., Papaioannou, A., Klein, K.-L., Afanasiev, A., Agueda, N., Aurass, H., Battarbee, M., Braune, S., Dröge, W., Ganse, U., Hamadache, C., Heynderickx, D., Huttunen-Heikinmaa, K., Kiener, J., Kilian, P., Kopp, A., Kouloumvakos, A., Maisala, S., Mishev, A., Miteva, R., Nindos, A., Oittinen, T., Raukunen, O., Riihonen, E., Rodríguez-Gasén, R., Saloniemi, O., Sanahuja, B., Scherer, R., Spanier, F., Tatischeff, V., Tziotziou, K., Usoskin, I.G., Vilmer, N.: 2013, The first SEPServer event catalogue ∼68-MeV solar proton events observed at 1 AU in 1996 – 2010. *J. Space Weather Space Clim.* **3**(27), A12. DOI.